Dual-Band Bandpass Filter With Independently Tunable Center Frequencies and Bandwidths

Girdhari Chaudhary, *Student Member, IEEE*, Yongchae Jeong, *Senior Member, IEEE*, and Jongsik Lim, *Senior Member, IEEE*

***Abstract*—This paper presents a novel approach to the design of tunable dual-band bandpass filter (BPF) with independently tunable passband center frequencies and bandwidths. The newly proposed dual-band filter principally comprises two dual-mode single band filters using common input/output lines. Each single BPF is realized using a varactor-loaded transmission-line dual-mode resonator. The proposed filter also offers switchable characteristics to select either of the passbands (either the first or the second passband only). To suppress the harmonics over a broad bandwidth, defected ground structures are used at input/output feeding lines without degrading the passbands characteristics. From the experimental results, it was found that the proposed filter exhibited the first passband center frequency tunable range from 1.48 to 1.8 GHz with a 3-dB fractional bandwidth (FBW) variation from 5.76% to 8.55% and the second passband center frequency tunable range from 2.40 to 2.88 GHz with the 3-dB FBW variation from 8.28% to 12.42%. The measured harmonic results of the proposed filters showed a rejection level of 19 dB, which is up to more than ten times of the highest center frequency of the first passband without degradation of the passbands.**

***Index Terms*—Defected ground structure (DGS), dual-band, harmonics suppression, tunable bandpass filter, varactor diode.**

I. Introduction

In the process of rapid evolution into microwave wireless communication, the demand for multiband/multifunctional microwave systems that support various modern services has increased rapidly. Such systems require microwave circuits and components that can handle several different frequency bands and bandwidths.

To meet these requirements, the design of multiband bandpass filters with tunable center frequency and bandwidths is essential due to their potential to significantly reduce system size and complexity. In this context, various approaches have been applied to design tunable bandpass filters (BPFs) using different kinds of tuning devices, such as micro-electromechanical system (MEMS) devices [1]–[4], ferroelectric devices/capacitors [5], [6], piezoelectric transducers [7], p-i-n diodes [8], and semiconductor varactor diodes [9]–[14].

These tuning devices allow a tunability of center frequency of filters by changing the effective length of their resonators and the variation of bandwidth by changing coupling between resonators.

The semiconductor varactors are widely used in designing tunable BPFs due to high tuning speed and reliability [9]–[14]. In comparison with the design of single-band tunable filters, only a limited number of efforts have been made in designing filters with tunable center frequency and bandwidth independently [15]–[20]. There have been some attempts to design tunable dual-passband filters [21]–[26]. However, none have addressed the design of independently controlled center frequencies and bandwidths.

With the tunable passband frequency, the harmonic bands that degrade the out-of-passband characteristics are also tuned. Thus, the suppression of harmonics is one of the critical issues for the tunable filters [27]–[29]. This issue has rarely been addressed in the design of tunable dual-band filters. There have been a few dual-band filters having fixed passbands incorporated with an extension of the upper stopband rejection characteristics [30]–[32]. In [30], the distances among the higher order resonances of hairpin resonators were limited so that the stopband performances needed improving. End-coupled stepped impedance resonators were used in [31] to achieve an excellent stopband rejection. In [32], multiple transmission zeros were incorporated in order to obtain broadband harmonic suppression.

In this paper, dual-band BPFs with independently tunable passband center frequencies and bandwidths are presented. From theoretical even- and odd-mode analysis, it is found that the passband center frequencies can be varied by controlling odd-and even-mode resonant frequencies. The separation between odd- and even-mode resonant frequencies are proportional to the bandwidth of passbands which can be controlled independently by even-mode resonant frequencies by keeping odd-mode resonant frequencies constant. To suppress the harmonics, the defected ground structure (DGS) is used at input/output feeding lines. The band-rejection characteristics of DGS are utilized to suppress the harmonics of the proposed BPF.

This paper is organized as follows. First, the characteristics of proposed tunable resonators are discussed in Section II. Second, the design and implementation of the filters along with the sim-

Manuscript received May 06, 2012; revised September 06, 2012; accepted September 13, 2012. Date of publication November 16, 2012; date of current version January 17, 2013.

G. Chaudhary and Y. Jeong are with the Department of Electronics and Information Engineering, IT Convergence Research Center, Chonbuk National University, Jollabuk-do 561-756, Korea (e-mail: ycjeong@jbnu.ac.kr).

J. Lim is with Soonchunhyang University, Chungcheongnam-do 336-745, Korea.

Color versions of one or more of the figures in this paper are available online at http://ieeexplore.ieee.org.

Digital Object Identifier 10.1109/TMTT.2012.2222910

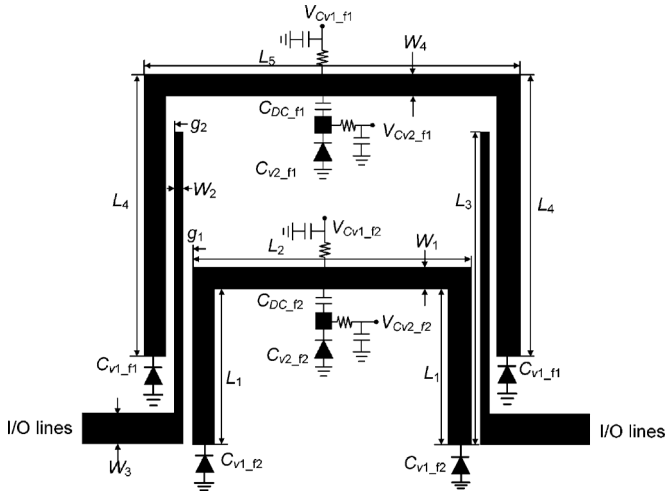

Fig. 1. Layout of the proposed two-pole dual-band tunable filter I.

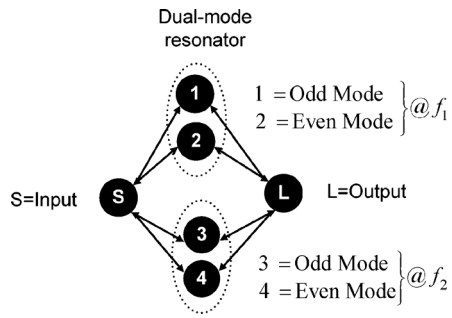

Fig. 2. Coupling scheme of the proposed filter I.

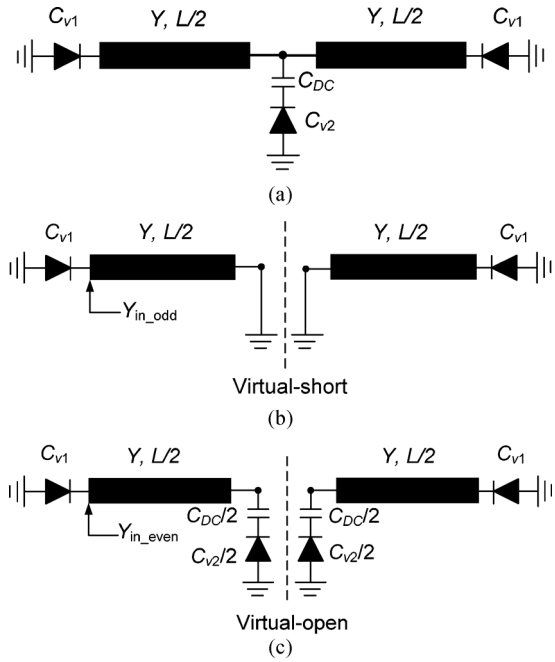

Fig. 3. (a) Basic structure of the proposed resonator. (b) Odd-mode excitation equivalent circuit. (c) Even-mode excitation equivalent circuit.

ulation and measurement results are described in Section III, followed by the conclusion in Section IV.

II. Theory and Design Equations

Fig. 1 shows the proposed two-pole varactor-tuned dual-band BPF. It consists of two single-band BPFs combined with common input and output ports. Each single-band BPF comprises dual-mode resonators that contain a transmission line and three varactor diodes. The coupling scheme of the proposed filter is shown in Fig. 2, where S and L denote input and output ports. Nodes 1 and 3 denote odd modes and nodes 2 and 4 denote even modes at the first (f_1) and second passband (f_2) center frequencies, respectively. Since these two operating modes do not couple to each other, a simple tuning scheme can be obtained.

A. Characteristics of Proposed Resonator

Fig. 3(a) shows the basic structure of the proposed resonator. Two varactor diodes are attached at ends of the transmission line with tunable capacitances C_{v1} and one varactor diode with tunable capacitance C_{v2} is placed at a center point of the transmission line. The dc block capacitor is placed at the center point of the transmission. For the theoretical analysis, the lossless transmission line of characteristic admittance Y and physical length L is assumed. Since the structure is symmetrical, the even- and odd-mode analysis method is applicable to obtain the resonant frequencies [26]. When the odd-mode excitation is applied to the ends of the proposed resonator shown in Fig. 3(a), there is a voltage null along the symmetry plane. Under the odd-mode excitation, it can be represented by the half circuit as shown in Fig. 3(b). The odd-mode input admittance is given as follows:

$$Y_{\text{in\_odd}} = j\left[\omega_{\text{odd}} C_{v1} - Y\cot\left(\frac{\beta L}{2}\right)\right] \tag{1}$$

where C_{v1} is the capacitance of the varactor diode connected at the end of the line and β is the propagation constant of the transmission line.

From the resonance condition of $\text{Im}(Y_{\text{in-}odd}) = 0$, the odd-mode resonant frequency can be determined as follows:

$$f_{\text{odd}} \times \tan\left(\frac{\pi f_{\text{odd}} L}{v_p}\right) = \frac{Y}{2\pi C_{v1}} \tag{2}$$

where v_p is the phase velocity. From (2), it is concluded that the odd-mode resonant frequency fully depends on the capacitance C_{v1} of the varactor diode connected at the ends of the transmission line. Moreover, the odd-mode resonant frequencies are not affected by the varactor diode connected at the center of the transmission line.

For the even-mode excitation, there is no current flowing through the center of the transmission line. Under the even-mode condition, the proposed resonator can be represented by the equivalent half circuit shown in Fig. 3(c). The even-mode input admittance is given as follows:

$$Y_{\text{in\_even}} = j\left(\omega_{\text{even}} C_{v1} + Y\frac{\omega C_{v2\_t} + Y\tan\left(\frac{\beta L}{2}\right)}{Y - \omega\tan\left(\frac{\beta L}{2}\right)C_{v2\_t}}\right) \tag{3}$$

where C_{v2_t} is the total capacitance for series connection of dc block capacitor and varactor diode, which is given as follows:

$$C_{v2\_t} = \frac{1}{2}\frac{C_{v2}C_{\rm DC}}{C_{v2}+C_{\rm DC}} \tag{4}$$

where C_{v2} and $C_{\rm DC}$ are the capacitance of the varactor diode and dc block connected at the center of the transmission line. For the resonance condition, the even-mode resonant frequency can be determined as follows:

$$\left(f_{\rm even} - \frac{Y^2}{4\pi^2 f_{\rm even} C_{v1} C_{v2\_t}}\right)\tan\left(\frac{\pi f_{\rm even} L}{v_p}\right) = Y\frac{C_{v1}+C_{v2\_t}}{2\pi C_{v1}C_{v2\_t}}. \tag{5}$$

From (4) and (5), it can be observed that the even-mode resonant frequency depends on C_{v1} and C_{v2}. Moreover, when C_{v1} is fixed, the even-mode resonant frequency can be tuned with C_{v2} alone. This characteristic of the proposed resonator can be used to design a BPF with tunable bandwidths.

In order to verify the theoretical analysis, a full-wave electromagnetic (EM) simulation was carried out using Ansoft's High Frequency Structural Simulator (HFSS) v11.

Two microstrip lines with characteristic impedance of 50 Ω were utilized to feed the proposed resonator using loose coupling to investigate its resonant behavior. The characteristic impedance of resonator are fixed at 76 Ω.

Fig. 4 shows the simulated S_{21}-magnitude of a weak coupling resonator circuit according to different capacitances (C_{v1} and C_{v2}) of varactor diodes and length (L). As C_{v1} and C_{v2} are varied, the odd- and even-mode resonant frequencies are tuned simultaneously. This characteristic of the proposed resonator can be utilized in the design of BPF with tunable passband center frequency. If capacitances C_{v1} of the varactor diodes connected at the end of the transmission line are fixed, it is obvious that the odd-mode resonant frequency is fixed and the even-mode resonant frequency can be tuned by varying the capacitance C_{v2} of the varactor diode connected at the center of the line. The separation between the modal frequencies is proportional to the bandwidth. This characteristic of proposed resonator can be utilized in the design of BPF with tunable bandwidths.

B. External Quality Factor (Q_e)

With I/O coupling, the circuit models for the odd and even modes are presented in Fig. 5. The external quality factor of odd ($Q_{\rm exo}$) and even modes ($Q_{\rm exe}$) of the proposed filter can be derived from the input reflection coefficient of the odd and even modes [13] as follows:

$$Q_{\rm exo} = \pi f_{\rm odd}\tau_{S11\_\rm odd} \tag{6a}$$

$$Q_{\rm exe} = \pi f_{\rm even}\tau_{S11\_\rm even} \tag{6b}$$

where $\tau_{S11-\rm odd}$ and $\tau_{S11-even}$ are group delays of S_{11} at the odd- and even-modes resonant frequencies, respectively.

Fig. 6 shows the extracted external quality factors for the first and second passbands under different g_1 and g_2 which are gaps between resonator and I/O lines. As g_1 and g_2 are increased, the external quality factors also increased. To maintain the shape and bandwidth of odd- and even-mode frequency responses, the external quality factors for the odd and even mode should vary with tuning frequency. As seen from Fig. 6, the odd-mode external quality factor can be controlled by C_{v1} only, whereas the even-mode external quality factor can be varied by both C_{v1} and C_{v2}. Therefore, from these graphs, values of g_1, g_2, and L_3 can be determined to meet the design specifications of the filter.

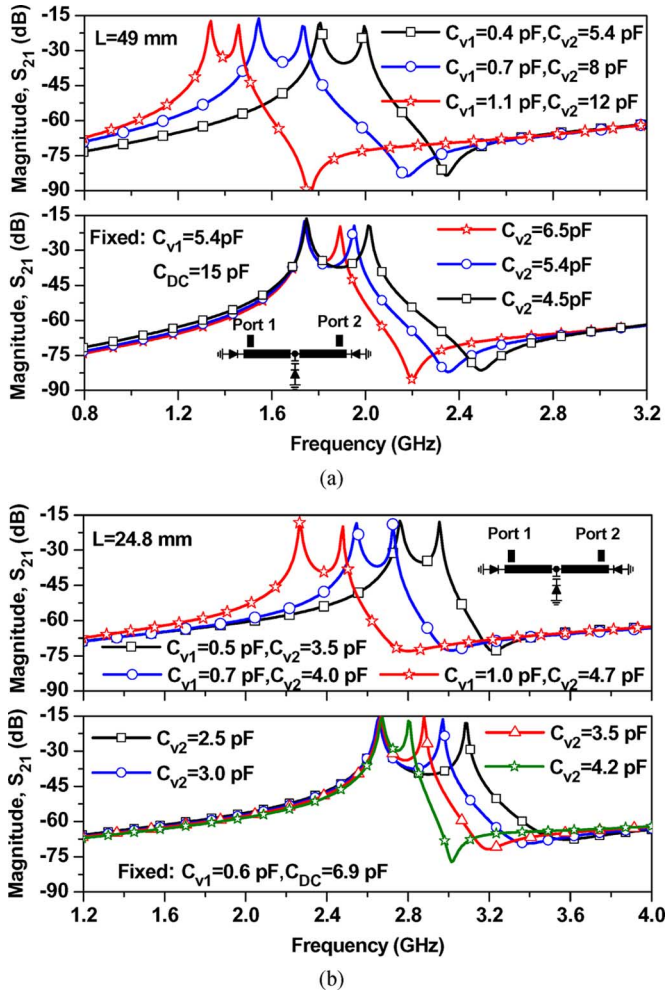

Fig. 4. Resonant frequencies of single dual-mode resonator according to capacitances and length at : (a) first passband and (b) second passband.

C. Design Method

First, the requirement of the ideal dual-mode tunable filter at each passband must be determined, which may be derived from its fixed frequency response centering at the high-frequency edge of a given tuning range. Then, separation of odd- and even-mode resonant frequencies and the required $Q_{\rm exo}$ and $Q_{\rm exe}$ for an ideal tunable filter can be determined at each passband as described in [13]. Second, the tuning rate of the odd-and even-mode resonant frequencies should be determined by selecting Y, L, C_{v1}, and C_{v2} by using (2) and (5) at each passband separately. Third, the coupling network should be designed to maintain the shape and bandwidth of odd- and even-mode frequency responses over the tuning range by properly choosing g_1, g_2, and L_3 according to the ideal requirement of the filter response.

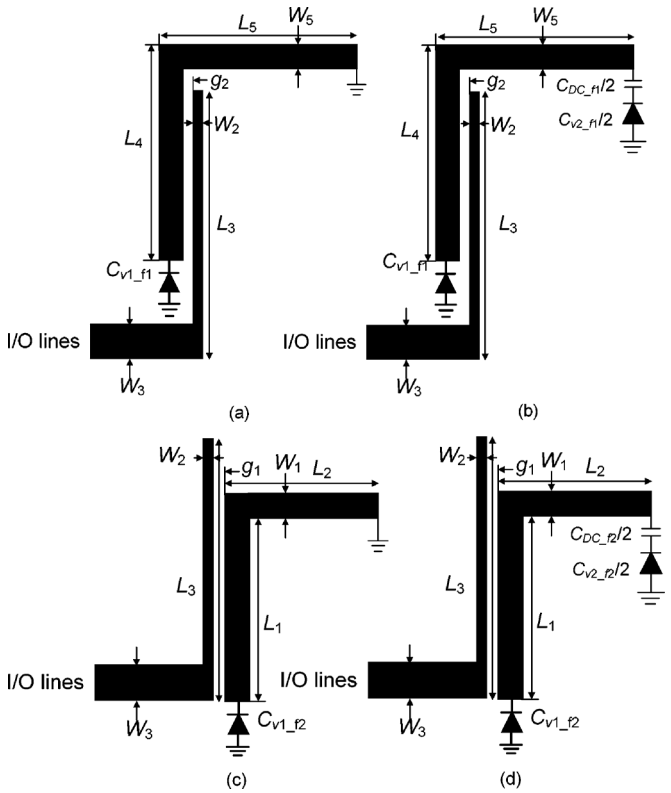

Fig. 5. Circuit model of (a) odd mode at first band, (b) even mode at the first passband, (c) odd mode at the second band, and (d) even mode at the second passband with I/O coupling.

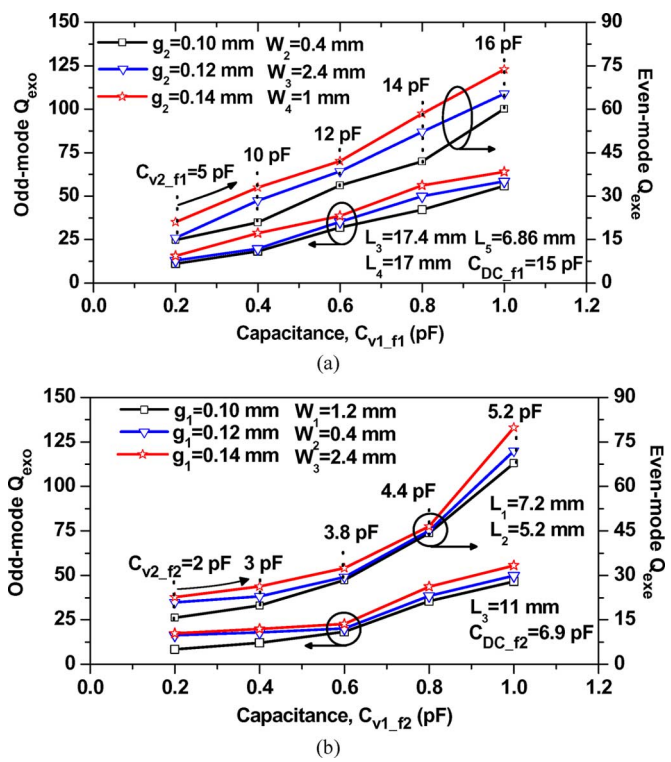

Fig. 6. Extracted external quality factors at (a) first passband and (b) second passband. Refer to Fig. 5 for notation.

To demonstrate the described design method, a filter centering at $f_1 = 1.80$ GHz and $f_2 = 2.9$ GHz with 3-dB FBWs of 5.8% and 9.5% has been designed, respectively. The desired parameters can be derived from a target-coupling matrix corresponding to specified response [33], which are given as $f_{\mathrm{odd-f1}} = 1.74$ GHz, $f_{\mathrm{even-f1}} = 1.94$ GHz, $Q_{\mathrm{exo-f1}} = 20.5$ and $Q_{\mathrm{exe-f1}} = 40.2$ at lower passband (f_1) and $f_{\mathrm{odd-f2}} = 2.76$ GHz, $f_{\mathrm{even-f2}} = 3.04$ GHz, $Q_{\mathrm{exo-f2}} = 23.5$ and $Q_{\mathrm{exe-f2}} = 29.5$ at higher passband (f_2). With these design parameters, the length and characteristic impedance of resonators at the first (f_1) and second (f_2) passband are chosen as 51 mm, 24.8 mm, and 76 Ω, respectively. Also, according to the external quality factors, the values of g_1, g_2, W_2, and L_3 are taken as 0.12, 0.14, 0.4, and 17.5 mm from Fig. 6, respectively.

D. Analysis of Center Frequency and Bandwidth Tunability

To tune the center frequency with constant filter response and bandwidth, two factors needed to be considered. First, the resonant frequencies of odd and even modes should be shifted proportionally. Second, external quality factors for odd and even modes should vary directly with tuning frequency. Similarly, the separation between the odd- and even-mode resonant frequencies are proportional to the bandwidth tunability while keeping the center frequency of passbands constant. Therefore, the filter bandwidth can be tuned by properly tuning the value of C_{v2} while keeping constant the value of C_{v1}. To demonstrate how to achieve this, the simulated results are plotted in Fig. 7.

Fig. 7(a) presents tunability of the center frequency of passbands according to capacitances ($C_{v1-\mathrm{f1}}$, $C_{v2-\mathrm{f1}}$, $C_{v1-\mathrm{f2}}$, and $C_{v2-\mathrm{f2}}$). The first passband center frequency (f_1) can be tuned from 1.4 to 1.82 GHz by adjusting $C_{v1-\mathrm{f1}}$ from 0.4 to 0.9 pF and $C_{v2-\mathrm{f1}}$ from 5.1 to 10.2 pF.

Similarly, the second passband center frequency (f_2) can be varied from 2.26 to 3 GHz by changing $C_{v1-\mathrm{f2}}$ from 0.4 to 0.9 pF and $C_{v2-\mathrm{f2}}$ from 2.2 to 6.7 pF.

Fig. 7(b) presents the 3-dB FBWs versus capacitances (fixing $C_{v1-\mathrm{f1}}$ and $C_{v1-\mathrm{f2}}$ and varying $C_{v2-\mathrm{f1}}$ and $C_{v2-\mathrm{f2}}$) for $f_1 =$ 1.53–1.82 and $f_2 =$ 2.38–3 GHz. From the simulation, it is found that the 3-dB FBW results in a tunable range of 5%–9% for $f_1 =$ 1.53–1.82 GHz and 6%–12% for $f_2 =$ 2.38–3 GHz.

III. Filter Implementation and Verification

To verify the analytical analysis of the proposed resonators, two types of tunable dual-band BPFs were designed, simulated, and measured.

Fig. 1 depicts the configuration of microstrip dual-mode tunable dual-band filter I. In the proposed filter, two dual-mode resonators are combined with common input/output ports. The inner resonators are designed for higher passbands, whereas the outer resonator is designed for lower passpbands. The resonators are folded in order to reduce the size. The substrate is RT/Duriod 5880 made by Rogers with a dielectric constant (ε_r) of 2.2 and thickness (h) of 31 mils.

The proposed filter employs two types of varactor diodes from Skyworks: SMV1231-011LF for tuning $C_{v1-\mathrm{f1}}$, and $C_{v1-\mathrm{f2}}$ and SMV1233-079LF for tuning of $C_{v2-\mathrm{f1}}$ and $C_{v2-\mathrm{f2}}$, respectively.

The Q values of the varactor diodes SMV1231-011LF and SMV1233-079LF are around 30–60 at 1.4–1.80 GHz and 50–70 at 2.4–3 GHz, respectively. After the simulation, the physical

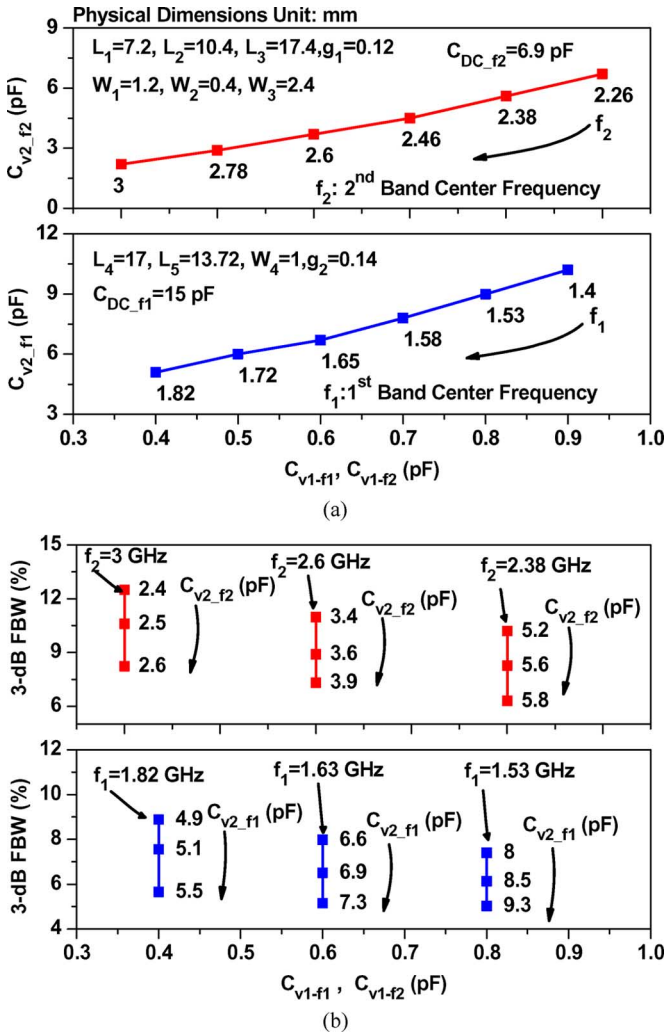

Fig. 7. Simulated results for tunability of center frequency and bandwidths of passbands according to capacitances. (a) Passbands center frequency tunability and (b) bandwidths tunability. Refer to Fig. 1 for notation.

TABLE I
DIMENSIONS FOR FABRICATED FILTER I (DIMENSIONS ARE IN MILLIMETERS). REFER TO FIG. 1 FOR NOTATION.

$W_1/W_2/W_3/W_4$	$L_1/L_2/L_3/L_4/L_5$	g_1/g_2	C_{DC_f1}/C_{DC_f2} [pF]
1.2/0.4/2.4/1	7.2/10.4/17.4/17/13.72	0.12/0.14	15/6.9

parameters and component values of the filter were determined, as shown in Table I.

A. Filter I: Tunable Center Frequencies

Fig. 8 shows the simulation and measurement results of filter I for several typical bias voltages. The measurement results agree well with the simulation results. The measurement results show that the first passband center frequency can be tuned from 1.48 to 1.8 GHz and the second passband center frequency can be tuned from 2.40 to 2.88 GHz. The return loss is better than 12 dB in the overall tuning range of both passbands. The insertion loss varies from 1.99 to 4.4 dB at the first passband, whereas it varied from 1.60 to 4.2 dB at the second passband. As the passbands are tuned towards lower frequencies, the insertion loss becomes higher. Because of decreasing bias voltages, the Q value of varactors becomes lower.

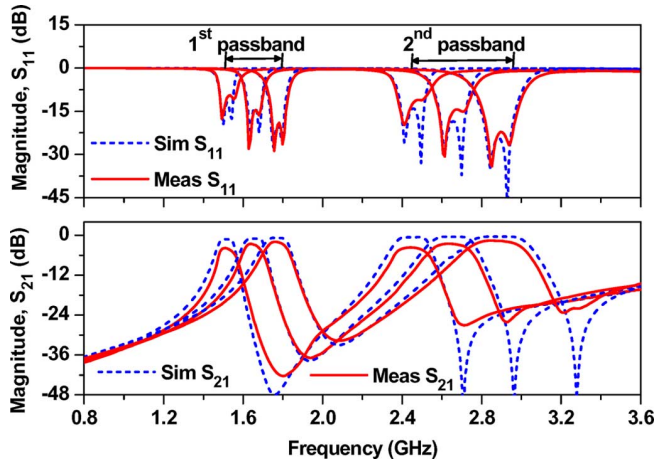

Fig. 8. Simulation and measurement results of filter I with tunable both passbands. Bias voltage variation: $V_{Cv1\_f1} = 3.78 \sim 15$ V, $V_{Cv2\_f1} = 0.59 \sim 15$ V, $V_{Cv1\_f2} = 4 \sim 15$ V, and $V_{Cv2\_f2} = 4 \sim 15$ V.

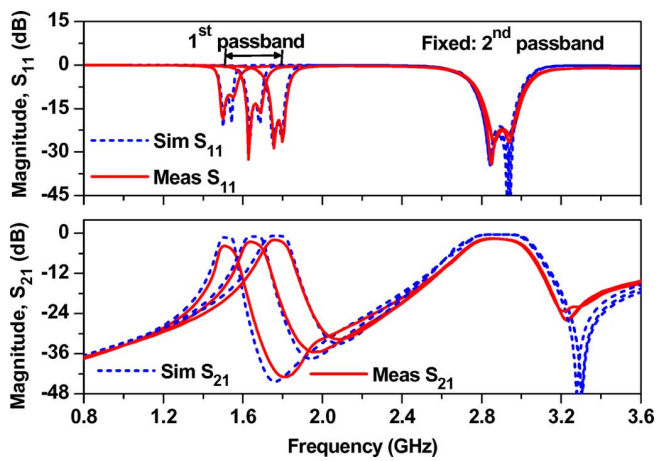

Fig. 9. Simulation and measurement results of filter I with tunable first passband and fixed second passband. Bias voltage variation: $V_{Cv1-f1} = 3.78 \sim 15$ V, $V_{Cv2-f1} = 0.59 \sim 15$ V, $V_{Cv1-f2} = 15$ V, and $V_{Cv2-f2} = 15$ V.

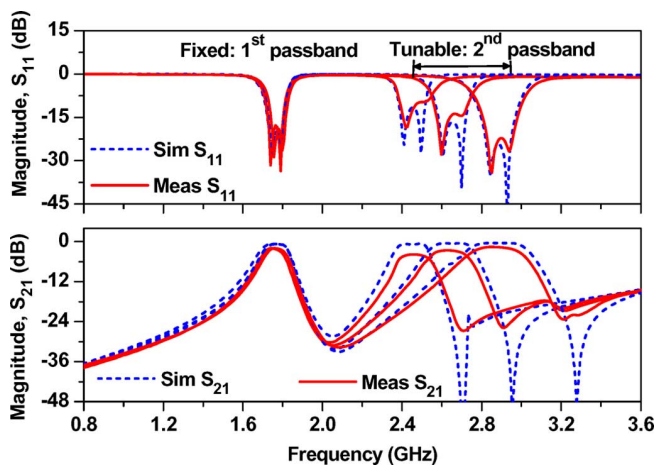

Fig. 10. Simulation and measurement results of filter I with fixed first passband and tunable second passband. Bias voltage variation: $V_{Cv1-f1} = 15$ V, $V_{Cv2-f1} = 15$ V, $V_{Cv1-f2} = 4 \sim 15$ V, and $V_{Cv2-f2} = 4 \sim 15$ V.

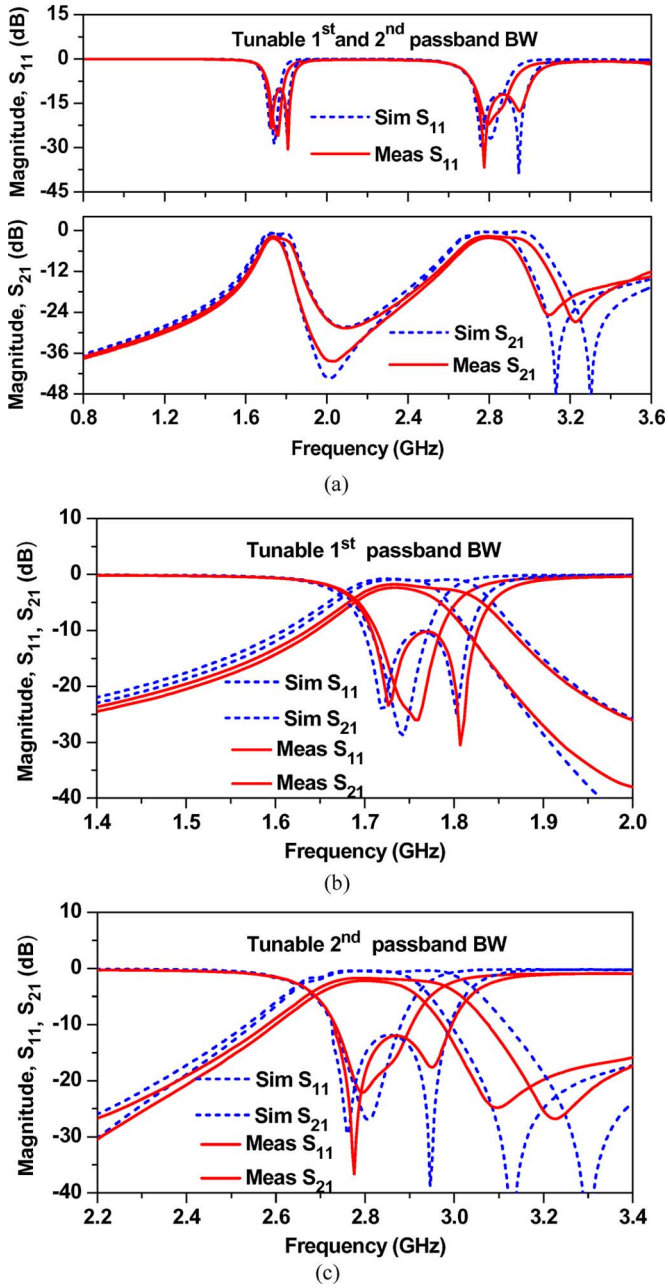

Fig. 11. Simulation and measurement results of filter I with tunable bandwidth of both passbands simultaneously. (a) Both passbands. (b) Magnified first band characteristics. (c) Magnified second band characteristics. Bias voltage variation: $V_{\mathrm{Cv1-f1}} = 15$ V, $V_{\mathrm{Cv2-f1}} = 6 \sim 15$ V, $V_{\mathrm{Cv1-f2}} = 15$ V, and $V_{\mathrm{Cv2-f2}} = 8 \sim 15$ V.

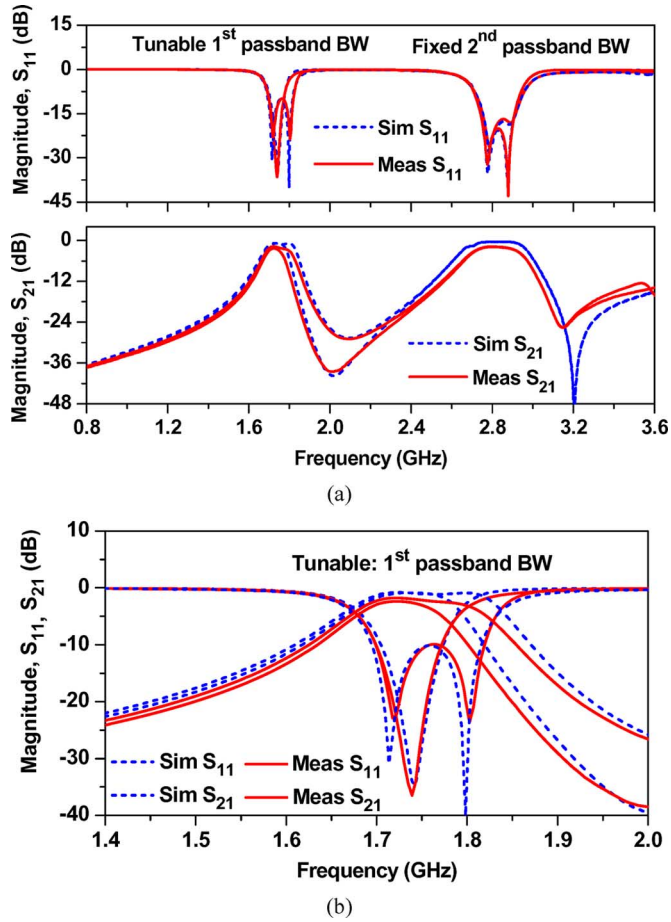

Fig. 12. Simulation and measurement results of filter I with fixed second passband bandwidth and tunable first passband bandwidth. (a) Both passbands. (b) Magnified first band characteristics. Bias voltage variation: $V_{\mathrm{Cv1\_f1}} = 15$ V, $V_{\mathrm{Cv2-f1}} = 6 \sim 15$ V, $V_{\mathrm{Cv1-f2}} = 15$ V, and $V_{\mathrm{Cv2-f2}} = 15$ V.

Fig. 9 shows the simulation and measurement results of filter I with the fixed second passband and tunable first passband center frequencies. The second passband center frequency is fixed at 2.88 GHz and the first passband center frequency is tuned from 1.48 to 1.8 GHz. The return loss is better than 12 dB over the entire tuning range of first passband. The insertion loss varies from 1.99 to 4.42 dB.

Fig. 10 shows the simulation and measurement results of filter I with the fixed first passband and tunable second passband center frequencies. The first passband center frequency is fixed at 1.74 GHz, and the second passband center frequency is tuned from 2.40 to 2.88 GHz with the return loss better than 12 dB over the entire tuning range. The insertion loss varies from 1.64 to 4.2 dB. From these results, it is clear that center frequencies of proposed filter can be tuned independently. However, the differences in insertion loss between the simulation and measurement results are due to the use of ideal capacitances in EM simulation.

B. Filter I: Tunable Bandwidths

Fig. 11 shows the simulation and measurement results of filter I with both tunable passband bandwidths. As seen in this figure, the first passband 3-dB FBWs can be tuned from 5.76% to 8.55% at 1.74 GHz and the second passband 3-dB FBW variation from 8.28% to 12.42% at the center frequency of 2.80 GHz, respectively. Figs. 12 and 13 show the simulation and measurement results of filter I to verify independently the tunable 3-dB FBWs of passbands. As seen in Fig. 12, the 3-dB FBW of the first passband is tunable with the fixed second passband bandwidth. Similarly, Fig. 13 shows the simulation and measurement results for the tunable 3-dB FBWs of the second passband with the fixed first passband bandwidth.

C. Filter I: Passband Switchable Characteristics

The proposed filter also offers the switchable passband characteristics, as shown in Fig. 14. By varying the capacitances of varactor diodes, either only the first or the second passband

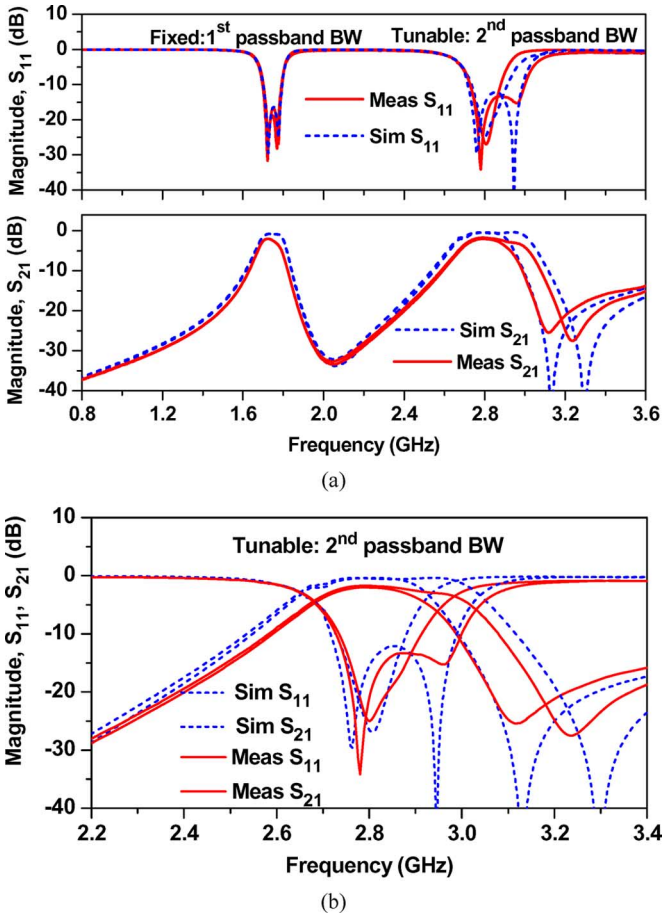

Fig. 13. Simulation and measurement results of filter I with fixed first passband bandwidth and tunable second passband bandwidth. (a) Both passbands. (b) Magnified second band characteristics. Bias voltage variation: $V_{\mathrm{Cv1\_f1}} = 15$ V, $V_{\mathrm{Cv2-f1}} = 15$V, $V_{\mathrm{Cv1-f2}} = 15$ V, and $V_{\mathrm{Cv2-f2}} = 8 \sim 15$ V.

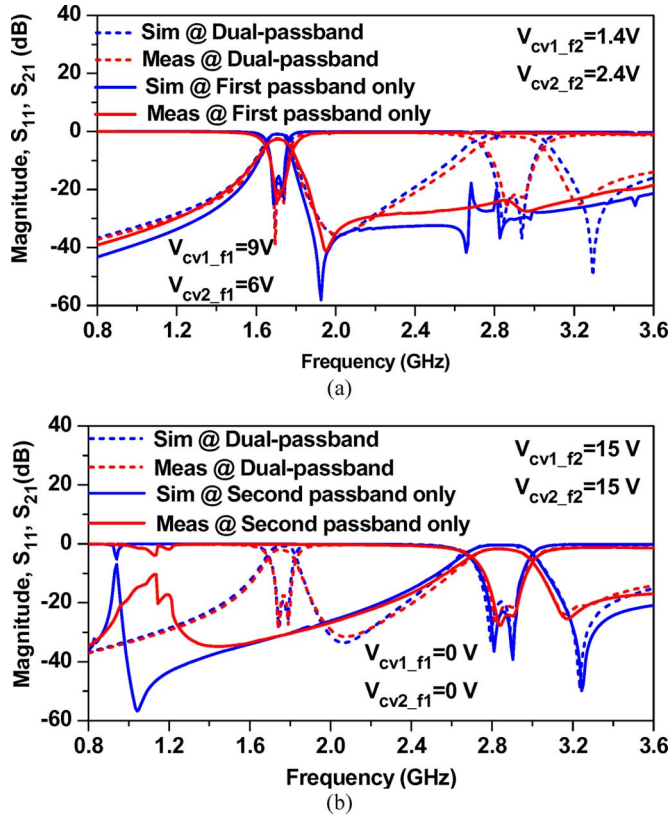

Fig. 14. Simulation and measurement results of filter I with passband switchable characteristics. (a) First passband only. (b) Second passband only.

can be selected. The first passband can be only selected by tuning the second passband odd- and even-mode resonant frequencies toward lower frequencies. Similarly, the second passband can be only selected by tuning the first passband odd- and even-mode resonant frequencies toward lower frequencies. However, the complete removal of the passband could not be performed because the varactor diode capacitances were not sufficiently high, as we required theoretically. While tuning odd- and even-mode resonant frequencies toward lower frequencies, the required coupling coefficient and external quality factors can not be obtained, which eliminates the passbands. The photograph of fabricated filter I is shown in Fig. 15.

D. Filter II: Tunable Dual-Band Bandpass Filter With Harmonic Suppression

It can be found from the simulation and measurement results in the previous section that there are several harmonics of the two passbands. These harmonics are also tuned by varying the passband frequencies and must be suppressed for the overall system performances. A simple method of suppressing the harmonics is to introduce a transmission zero at the harmonic frequency [34]. However, this method would be inefficient, because it can only suppress the harmonics around a specific frequency. Due to a broad range of variation of the harmonic frequency in the case of the tunable dual-band BPF, it is not possible to cancel harmonics sufficiently by a simple transmission zero circuit.

The DGS of the microstrip line is implemented by making artificial defects on the ground plane and provides band-rejection characteristics corresponding to the size and shape of defects on the ground plane.

The DGS also provides an additional effective inductance in the transmission line, which enables the slow-wave factor of the line to be increased. These band-rejection properties and slow-wave effect of DGS have been applied in the design of various microwave circuits such as filters, dividers, and amplifiers [35]–[37]. In microwave circuits, the band-rejection property of the DGS can also be utilized in the suppression of harmonics [26], [38]–[41].

Fig. 16 shows the proposed configuration of the harmonic-suppressed tunable dual-band filter II. In this structure, DGS is used at the input/output feeding lines for inducting coupling and acts as the broad band-rejection resonator to suppress the harmonics of filter I. The methods for finding the equivalent circuits of DGS are detailed in [35]. The physical parameters and component values of filter II are shown in Table II.

Fig. 17(a) shows narrowband characteristics of the simulation and measurement results of filter II. The passband frequencies are controlled with the help of the bias voltages of the varactor diodes. From the measurement results, the first passband frequency can be tuned from 1.5 to 1.8 GHz. and the second passband frequency can be tuned from 2.45 to 2.80 GHz. The return loss is better than 11 dB over the entire tuning range of the passbands. The insertion loss varies from 3.02 to 4.8 dB at the first

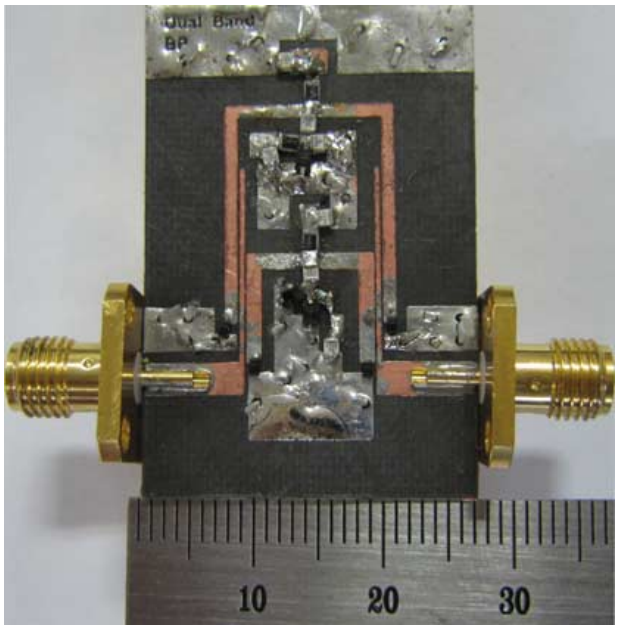

Fig. 15. Photograph of fabricated filter I.

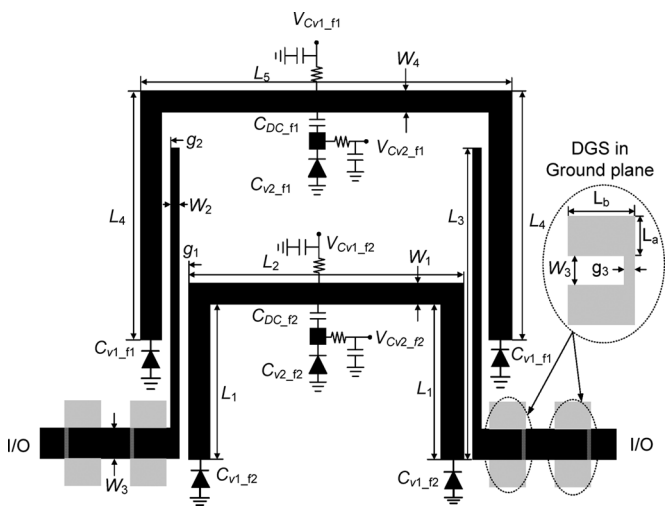

Fig. 16. Configuration of filter II.

TABLE II
DIMENSIONS FOR FABRICATED FILTER II (DIMENSIONS ARE IN MILIMETERS). REFER TO FIG. 16 FOR NOTATION..

$W_1/W_2/W_3/W_4$	$L_1/L_2/L_3/L_4/L_5/L_a/L_b$	$g_1/g_2/g_3$	C_{DC_f1}/C_{DC_f2} [pF]
1.2/0.4/2.4/1	7.2/10.4/17.4/17/13.7/5/4	0.12/0.14/0.28	15/6.9

passband and from 2.78 to 4.6 dB at the second passband. These measurement results for filter II are almost similar to filter I results in the previous section except for the suppression of the harmonic characteristics.

In order to verify the harmonic suppression characteristics of filter II, the broadband harmonic suppression characteristics are shown in Fig. 17(b). The harmonic suppression characteristics for the fabricated filter II are better than 19 dB up to 18 GHz over

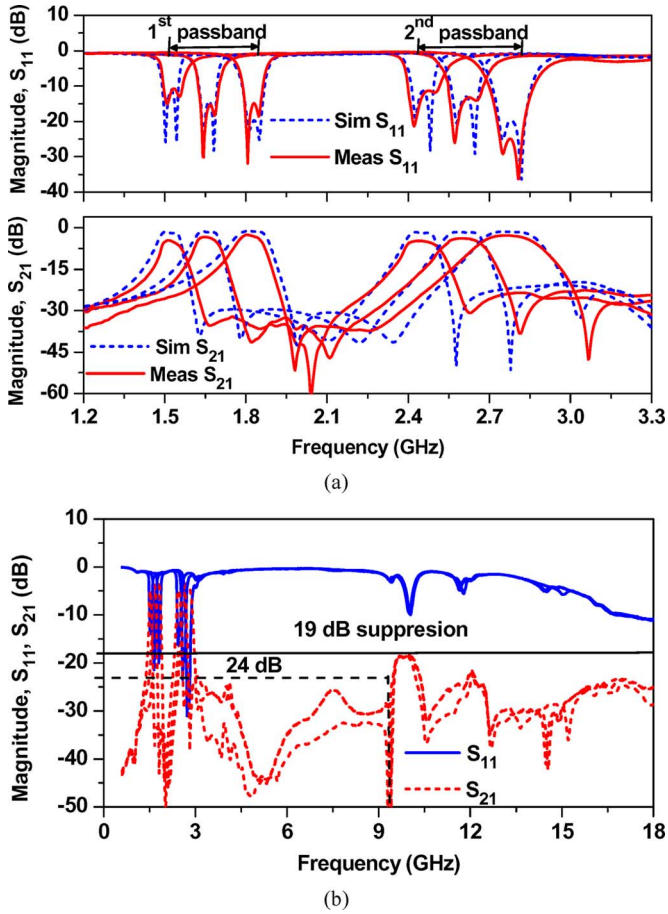

Fig. 17. Simulation and measurement results of filter II with tunable both passbands. (a) Narrowband and (b) wideband characteristics. Bias voltage variation: $V_{Cv1\_f1} = 4.09 \sim 13$ V, $V_{Cv2-f1} = 0.93 \sim 15$ V, $V_{Cv1-f2} = 5.60 \sim 15$ V, and $V_{Cv2-f2} = 3.21 \sim 15$ V.

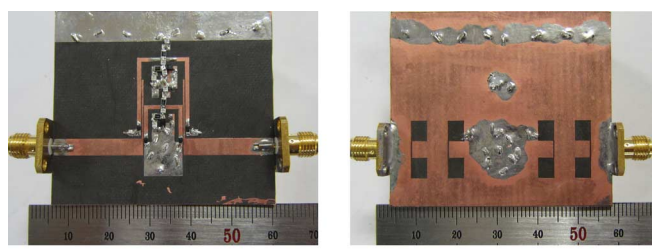

(a) (b)

Fig. 18. Photograph of fabricated filter II. (a) Top view. (b) Bottom view.

the entire tuning range of the passbands. This means that the proposed structure can suppress more than tenth-order harmonics of the highest center frequency of the first passands due to the band-rejection characteristics of DGS. This confirmed that the proposed method can achieve broadband harmonic suppression without degrading any passband performances. However, the spurious response occurs around 10 GHz, which is not completely suppressed by band-rejection characteristics the DGS.

The photographs of the fabricated filter II are shown in Fig. 18. Performance comparisons of the proposed tunable filter with other tunable filters reported in the literature are summarized in Table III. The proposed filter can provide

TABLE III
PERFOMANCE COMPARISON OF TUNABLE FILTERS WITH INDEPENDENT CONTROL OF CENTER FREQUENCY AND BANDWIDTH.

	Frequency Tunability [GHz]		3-dB FBW Tunability [%]		A	Harmonic Suppression Order
	f_1	f_2	f_1	f_2		
[12]	0.85-1.40	x	2.9-5.2*	x	N	x
[15]	1.50-2.20	x	2.2-12.2*	x	Y	x
[16]	1.75-2.25	x	4-5.71*	x	Y	x
[17]	2.90-3.50	x	4-12	x	Y	x
[18]	0.47-0.862	x	1.06-3.19	x	Y	x
[20]	3.70-6.0**	x	1.6-9.3*	x	Y	x
[25]	2.20-2.70	3.45-4.20	x	x	N	-20 dB up to 1.75 f_{2_max}
[26]	0.85-1.20	1.40-2.14	x	x	N	-20 dB more than 10 f_{2_max}
This work	**1.48-1.80**	**2.40-2.88**	**5.7-8.5**	**8.2-12.4**	**Y**	**-19 dB more than to 10f_{1_max}**

A= Independently tunable center frequency and bandwidth
Y/N=Yes/No
*=1-dB FBW
**=Suspended-striplinerings in MEMS technology
f_{1_max}= Highest center frequency of first passband
f_{2_max}= Highest center frequency of second passband

dual passbands with independently tunable center frequencies and bandwidths in addition to broadband harmonic-rejection characteristics.

IV. CONCLUSION

In this paper, the design of tunable dual-band BPFs with independently tunable center frequencies and bandwidths are demonstrated. The proposed structure is validated by both theoretical analysis and experiments. The defected ground structures are utilized to reject harmonics. The experimental results are in good agreement with the theoretical predictions. The experimental results showed that the first passband can be tuned from 1.48 to 1.8 GHz with the 3-dB fractional bandwidth tunability of 5.76%–8.55% and the second passband can be tuned from 2.40 to 2.88 GHz with the 3-dB fractional bandwidth tunability of 8.25%–12.42%. The proposed filter also offers passband-switchable characteristics. The proposed method can suppress more than tenth-order harmonics of second passbands, thereby ensuring the broad harmonic-rejection characteristics without any degradation of passband characteristics. The proposed filter design method can be applicable to selectable multimode or multiband applications that have different operating frequencies and bandwidths.

REFERENCES

[1] K. Entesari and G. M. Rebeiz, "A differential 4-bit 6.5–10 GHz RF MEMS tunable filter," *IEEE Trans. Microw. Theory Tech.*, vol. 53, no. 3, pp. 1103–1110, Mar. 2005.

[2] S. Park, M. A. El-Tanani, I. Reines, and G. M. Rebeiz, "Low-loss 4–6 GHz tunable filter with 3-bit high Q-orthogonal bias RF-MEMS capacitance network," *IEEE Trans. Microw. Theory Tech.*, vol. 56, no. 10, pp. 2348–2355, Oct. 2008.

[3] F. Huang, S. Fouladi, and R. Mansour, "High Q-tunable dielectric resonator filters using MEMS technology," *IEEE Trans. Microw. Theory Tech.*, vol. 59, no. 12, pp. 3401–3409, Dec. 2011.

[4] K. Entersari and G. M. Rebeiz, "A 12–18 GHz three-pole RF MEMS tunable filter," *IEEE Trans. Microw. Theory Tech.*, vol. 53, no. 8, pp. 2566–2571, Aug. 2005.

[5] J. Nath, D. Ghosh, J. P. Maria, A. I. Kingon, W. Fathelbab, P. D. Franzon, and M. B. Steer, "An electronically tunable microstrip bandpass filter using thin-film barium-strontium-titante (BST) varactors," *IEEE Trans. Microw. Theory Tech.*, vol. 53, no. 9, pp. 2707–2712, Sep. 2005.

[6] H. Jiang, B. Lacroix, K. Choi, Y. Wang, and A. T. H. Papapolymerou, "Ka- and U-band tunable bandpass filters using ferroelectric capacitors," *IEEE Trans. Microw. Theory Tech.*, vol. 59, no. 12, pp. 3068–3074, Dec. 2011.

[7] L. H. Hsieh and K. Chang, "Tunable microstrip bandpass filters with two transmission zeros," *IEEE Trans. Microw. Theory Tech.*, vol. 51, no. 2, pp. 520–525, Feb. 2003.

[8] B. Liu, F. Wei, and X. Shi, "Reconfigurable bandpass filter based on net-type stepped impedance resonator," *Electron. Lett.*, vol. 46, no. 22, pp. 1506–1507, Feb. 2010.

[9] I. C. Hunter and J. D. Rhodes, "Electronically tunable microwave band pass filters," *IEEE Trans. Microw. Theory Tech.*, vol. MTT-30, no. 9, pp. 1354–1360, Sep. 1982.

[10] B. W. Kim and S. W. Yun, "Varactor tuned combline bandpass filter using step-impedance microstrip lines," *IEEE Trans. Microw. Theory Tech.*, vol. 52, no. 4, pp. 1279–1283, Apr. 2004.

[11] A. R. Brown and G. M. Rebeiz, "A varactor tuned RF filter," *IEEE Trans. Microw. Theory Tech.*, vol. 48, no. 7, pp. 1157–1160, Jul. 2000.

[12] S. J. Park and G. M. Rebeiz, "Low loss two pole tunable filters with three different predefined bandwidth characteristics," *IEEE Trans. Microw. Theory Tech.*, vol. 56, no. 5, pp. 1137–1148, May 2008.

[13] W. Tang and J. Hong, "Varactor-tuned dual-mode bandpass filters," *IEEE Trans. Microw. Theory Tech.*, vol. 58, no. 8, pp. 2213–2219, Aug. 2010.

[14] J. Long, C. Li, W. Cui, J. Huangfu, and L. Ran, "A tunable microstrip bandpass filter with two independently adjustable transmission zeros," *IEEE Microw. Wireless Compon. Lett.*, vol. 21, no. 2, pp. 74–76, Feb. 2011.

[15] Y. Chiou and G. M. Rebeiz, "A tunable three-pole 1.5–2.2 GHz bandpass filter with bandwidth and transmission zero control," *IEEE Trans. Microw. Theory Tech.*, vol. 59, no. 11, pp. 2872–2878, Nov. 2011.

[16] Y. Chiou and G. M. Rebeiz, "A quasi elliptic function 1.75–2.25 GHz 3-pole bandpass filter with bandwidth control," *IEEE Trans. Microw. Theory Tech.*, vol. 60, no. 2, pp. 244–249, Feb. 2012.

[17] A. L. C. Serrano, F. S. Correra, T. P. Vuong, and P. Ferrari, "Synthesis methodology applied to a tunable path filter with independently frequency and bandwidth control," *IEEE Trans. Microw. Theory Tech.*, vol. 60, no. 3, pp. 484–493, Mar. 2012.

[18] M. Sanchez-Renedo, R. Gomez-Garcia, J. I. Alonso, and C. Briso-Rodriguez, "Tunable combline filter with continuous control of center frequency and bandwidth," *IEEE Trans. Microw. Theory Tech.*, vol. 53, no. 1, pp. 191–199, Jan. 2005.

[19] J. S. Sun, N. Keneda, Y. Baeyens, T. Itoh, and Y. K. Chen, "Multilayer planar tunable filter with very wide tuning bandwidth," *IEEE Trans. Microw. Theory Tech.*, vol. 59, no. 11, pp. 2864–2870, Nov. 2011.

[20] C. C. Cheng and G. M. Rebeiz, "High-Q 4–6 GHz suspended stripline RF MEMS tunable filter with bandwidth control," *IEEE Trans. Microw. Theory Tech.*, vol. 59, no. 10, pp. 2469–2476, Oct. 2011.

[21] X. Y. Zhang and Q. Xue, "Novel centrally loaded resonators and their applications to bandpass filters," *IEEE Trans. Microw. Theory Tech.*, vol. 56, no. 4, pp. 913–921, Apr. 2008.

[22] D. Girbau, A. Lazaro, E. Martinez, D. Masone, and L. Pradell, "Tunable dual-band bandpass filter for WLAN applications," *Microw. Opt. Technol. Lett.*, vol. 51, no. 9, pp. 2025–2028, Sep. 2009.

[23] D. Girbau, A. Lazaro, A. Parez, E. Martinez, L. Pradell, and R. Villarino, "Tunable dual-band filters based on capacitive loaded stepped impedance resonators," in *Proc. 39th Eur. Microw. Conf.*, 2009, pp. 113–116.

[24] G. Chaudhary, H. Choi, Y. Jeong, J. Lim, D. Kim, and J.-C. Kim, "Design of dual-band bandpass filter using DGS with controllable second passband," *IEEE Microw. Wireless Compon. Lett.*, vol. 21, no. 11, pp. 589–891, Nov. 2011.

[25] E. E. Djoumessi, M. Chaker, and K. Wu, "Varactor-tuned quarter-wavelength dual-bandpass filter," *IET Microw. Antenna and Propagat.*, vol. 3, no. 1, pp. 117–124, Feb. 2009.
[26] G. Chaudhary, Y. Jeong, and J. Lim, "Harmonic suppressed dual-band bandpass filters with tunable passbands," *IEEE Trans. Microw. Theory Tech.*, vol. 60, no. 7, pp. 2115–2123, Jul. 2012.
[27] H. J. Park, J. Y. Park, J. C. Lee, J. H. Kim, B. Lee, N. Y. Kim, and U. S. Hong, "A new varator tuned microstrip ring bandpass filter with harmonic suppression," in *Proc. Asia–Pacific Microw. Conf.*, 2000, pp. 1127–1130.
[28] X. Y. Zhang, Q. Xue, C. H. Chan, and B. J. Hu, "Low-loss frequency agile bandpass filters with controllable bandwidth and suppressed second harmonic," *IEEE Trans. Microw. Theory Tech.*, vol. 58, no. 6, pp. 1557–1564, Jun. 2010.
[29] X. Y. Zhang and Q. Xue, "High selectivity tunable bandpass filters with harmonic suppression," *IEEE Trans. Microw. Theory Tech.*, vol. 58, no. 4, pp. 964–969, Apr. 2010.
[30] M. Jiang, H. P. Lin, and J. T. Kuo, "Design of quasi-elliptic function filters with dual-passband responses with multi-spurious suppression," in *Proc. Asia–Pacific Microw. Conf.*, 2007, pp. 2365–2368.
[31] M. Mokhtaari, K. Rambabu, J. Bornemann, and S. Amari, "Advanced stepped-impedance dual-band filters with wide second stopbands," in *Proc. Asia–Pacific Microw. Conf.*, 2007, pp. 2285–2288.
[32] J. T. Kuo and H. P. Lin, "Dual-band bandpass filter with improved performances in extended upper rejection band," *IEEE Trans. Microw. Theory Tech.*, vol. 57, no. 4, pp. 824–829, Apr. 2009.
[33] A. Amari, U. Rosenberg, and J. Bornemann, "Adaptive synthesis and design of resonator filters with source/load-multiresonator coupling," *IEEE Trans. Microw. Theory Tech.*, vol. 50, no. 8, pp. 1969–1978, Aug. 2002.
[34] S. Sun and L. Zhu, "Periodically non-uniform coupled microstrip-line filter with harmonic suppression using transmission zero reallocation," *IEEE Trans. Microw. Theory Tech.*, vol. 53, no. 5, pp. 1817–1822, May 2005.
[35] D. Ahn, J. S. Park, C. S. Kim, J. N. Kim, Y. Qian, and T. Itoh, "A design of low-pass filter using the novel microstrip defected ground structure," *IEEE Trans. Microw. Theory Tech.*, vol. 49, no. 1, pp. 86–93, Jan. 2001.
[36] J. S. Lim, S. W. Lee, C. S. Kim, J. S. Park, D. Ahn, and S. Nam, "A 4:1 unequal Wilkinson power divider," *IEEE Microw. Wireless Compon. Lett.*, vol. 11, no. 3, pp. 124–126, Mar. 2001.
[37] Y. Jeong, S. Jeong, J. Lim, and S. Nam, "A new method to suppress harmonics using $\lambda/4$ bias line combined by defected ground structure in power amplifier," *IEEE Microw. Wireless Compon. Lett.*, vol. 13, no. 12, pp. 538–540, Dec. 2001.
[38] J. Park, J. Kim, and S. Nam, "Design of a novel harmonic suppressed microstrip low-pass filter," *IEEE Microw. Wireless Compon. Lett.*, vol. 17, no. 6, pp. 424–426, Jun. 2007.
[39] D. Woo and T. Lee, "Suppression of harmonics in Wilkinson power divider using dual-band rejection by asymmetric DGS," *IEEE Trans. Microw. Theory Tech.*, vol. 53, no. 6, pp. 2139–2144, Jun. 2005.
[40] C. Kim, D. Kim, I. Song, K. Leong, T. Itoh, and D. Ahn, "A design of a ring bandpass filters with wide rejection band using DGS and spur-line coupling structures," in *IEEE MTT-S Int. Microw. Symp. Dig.*, 2005, pp. 2183–2186.
[41] J. Lim, C. Kim, D. Ahn, Y. Jeong, and S. Nam, "Design of low-pass filters using defected ground structure," *IEEE Trans. Microw. Theory Tech.*, vol. 53, no. 8, pp. 2539–2545, Aug. 2005.

Girdhari Chaudhary (S'10) received the B.E. degree from Nepal Engineering College, Kathmandu, Nepal, in 2004, and the M.Tech degree from Malaviya National Institute of Technology, Jaipur, India, in 2007, both in electronics and communication engineering. He is currently working toward the Ph.D. degree at Chonbuk National University, Jeonju, Korea.

His research interests include multi-band passive circuits, negative group delay filters, and high-efficiency power amplifiers.

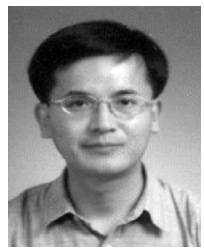

Yongchae Jeong (M'99–SM'10) received the B.S.E.E., M.S.E.E., Ph.D. degrees in electronics engineering from Sogang University, Seoul, Korea, in 1989 and 1991, respectively.

From 1991 to 1998, he was a Senior Engineer with Samsung Electronics. In 1998, he joined the Division of Electronic Engineering, Chonbuk National University, Jeonju, Korea. From July 2006 to December 2007, he was with the Georgia Institute of Technology, Atlanta, as a Visiting Professor. He is currently a Professor and member of the IT Convergence Research Center, Chonbuk National Univeristy. He has authored and coauthored over 100 papers in international journals and conference proceedings. He is currently teaching and conducting research in the areas of microwave devices, base-station amplifiers, nonlinear devices and system linerizing technology and RFIC design.

Dr. Jeong is a member of the Korea Institute of Electromagnetic Engineering and Science.

Jongsik Lim (S'90–M'93–SM'05) received the B.S. and M.S. degrees in electronic engineering from Sogang University, Seoul, Korea, in 1991 and 1993, respectively, and the Ph.D. degree in electrical engineering from Seoul National University, Seoul, in 2003.

In 1993, he joined ETRI, Daejeon, Korea, and was with them for six years in the Satellite Communication Division as a Senior Member of Research Staff. He was one of the key members in developing MMIC LNA and SSPA for 20/30 GHz satellite transponder in ETRI. From March to July in 2003, he was with the Division of Information Technology, Brain Korea 21 Project, Seoul National University, Seoul, as a Postdoctoral Fellow, and he gave lectures in the graduate schools of Soonchunhyang University and Soongsil University. He was a Patent Examiner with the Korean Intellectual Property Office (KIPO) from July 2003 to September 2004. In September 2004, he rejoined ETRI, where he was with the Antenna Technology Research Team/Radio Technology Group as a Senior Research Member. Since March 2005, he has been with the Department of Electrical and Communication Engineering, Soonchunhyang University, Chungcheongnam, Korea, as a Faculty Member. His current research interests include the design of the passive and active circuits for RF/microwave and millimeter-wave with MIC/MMIC technology, modeling of active devices, design of high-power amplifiers for mobile communications, applications of periodic structure to the RF/microwave circuits, and modeling of passive structure having periodic structures.

Dr. Lim is a member of the Institute of Electronic, Information and Communication Engineers of Japan and the Korea Institute of Electromagnetic Engineering and Science.